Magnetism of hexagonal 3*d* transition metals

Marek Podgórny
Instytut Fizyki, Uniwersytet Jagielloński, ul. Reymonta 4, PL-30-059 Kraków, Poland
and Institut für Theoretische Physik III, Ruhr Universität, Bochum, West Germany

Jacek Goniakowski
Instytut Fizyki, Uniwersytet Jagielloński, ul. Reymonta 4, PL-30-059 Kraków, Poland
(Received 8 January 1990)

The magnetic and mechanical equations of state and the total energy as functions of both magnetic moment and atomic volume have been self-consistently calculated using the linear muffin-tin orbital method within the fixed-spin-moment scheme for all 3*d* transition metals from Sc to Ni in a hexagonal structure. At zero pressure, Co and Ni ferromagnetic high-spin phases are found to be stable. Cr is found to be ferromagnetic with a very small magnetic moment that increases slowly and gradually with atomic volume. Mn and Fe are predicted to be metamagnetic; however, for Fe a stable high-spin ferromagnetic phase at rather low negative internal pressure is found. The light 3*d* transition metals (Sc, Ti, V) become magnetic only at very large lattice expansions. The electronic structure, the densities of states, and the total energies are discussed for the phases that may probably be produced by molecular-beam epitaxy.

I. INTRODUCTION

Molecular-beam epitaxy (MBE) has recently been used to produce new ferromagnetic materials. Prinz[1] was able to obtain ferromagnetic Co in a body-centered cubic structure and Maurer *et al.*[2] have succeeded in growing hexagonal ferromagnetic Fe. Also recently, an extensive effort has been undertaken to find theoretically the stability conditions of 3*d* (Refs. 3–6) and 4*d* (Ref. 7) magnetic cubic materials. These studies have used either the Stoner model[6] or the self-consistent electronic structure calculations in the fixed-spin-moment (FSM) mode.[8] A superiority of the latter approach seems to be indisputable as far as the accuracy of predictions and the abundance of outcoming information is involved.[3] However, the FSM calculations are computationally rather intensive and, as a consequence, until now they have remained restricted (with only a few exceptions) to the simplest bcc and fcc structures. The electronic structure of elemental hexagonal metals has been in general much less studied, probably due to a higher complexity of this lattice. No FSM study exists and the conventional floating-moment self-consistent calculations are not numerous. The electronic structure of the hexagonal Co has been studied by Jarlborg and Peter[9] with use of the linear muffin-tin orbital (LMTO) method. Recently, a thorough study of the electronic structure of all elemental metals (up to Cd) possessing a hexagonal structure in their ground states has been carried out by Blaha, Schwarz, and Dederichs.[10] Their paper can be consulted for a list of earlier (mostly not self-consistent) studies of the electronic structure of hexagonal metals.

In another very recent paper Papaconstantopoulos, Fry, and Brener[11] applied the Stoner theory to investigate ferromagnetic instabilities of all 3*d* transition metals in a hexagonal close packed (hcp) structure. Their calculations started from self-consistent nonmagnetic state densities of Sc, Ti, or Co and used the rigid-band model to calculate the density of states (DOS) at Fermi level for the remaining 3*d* transition metals. Combining these results with the values of Stoner exchange integral *I* tabulated by Janak[12] they predicted a ferromagnetic instability for hcp Co and Ni and suspected its existence for hcp Cr. They found other hcp 3*d* transition metals to be nonmagnetic. Surprisingly, their calculations gave no indication of ferromagnetism in hexagonal Fe, although it was recently discovered in experiment.[2] This happened because the analysis presented in Ref. 11 is somewhat incomplete. Conclusions drawn from the rigid-band approximation apply to the ground state of a considered material at some (not well defined) atomic volume that corresponds to the *d*-band width of the material the DOS of which served as input to the rigid-band calculation. The *d*-band width is inversely proportional to the fifth power of the lattice constants, the fact completely neglected within the rigid-band approximation. Papaconstantopoulos, Fry, and Brener[11] suggested inclusion of the Stoner integral volume dependence into their calculation. Since this dependence is known to be rather weak,[6] it is a second-order effect in comparison to the rigid-band model itself and its inclusion will not change much, unless the *d*-band width is scaled accordingly. The authors of Ref. 11 pointed out that a prospect for new magnetic materials produced by MBE in hcp phases appears to be excellent. It might be so and we will support this conclusion in certain cases but it seems to us that the information provided by the analysis carried out by Papaconstantopoulos, Fry, and Brener[11] is too scarce in order to discuss the issue. Since every 3*d* or 4*d* transition metal becomes either magnetic or nonmagnetic at certain atomic volumes,[5] the statement that a material is nonmagnetic and another one ferromagnetic is very im-

precise without taking into account a volume-dependence of magnetic moment. This dependence and the total energy and electronic pressure calculated along the stable branches of the $M(V)$ curve are of primary interest for experimentalists using the MBE technique. Such data can be in principle borne out by a Stoner-type analysis provided that at least the nonmagnetic electronic structure of a material is calculated self-consistently as a function of atomic volume.[6]

In this paper we assume a different strategy. We carry out the full-scale self-consistent LMTO calculations of all the quantities mentioned above and some other parameters for the whole series of $3d$ transition metals from Sc to Ni assuming a hexagonal structure. Only nonmagnetic and ferromagnetic phases are considered. The canonical scaling principle of the LMTO-ASA is employed in order to calculate the properties of the ferromagnetic phases within the FSM method. We point out which of the $3d$ hexagonal metals have a chance to be grown by MBE in the ferromagnetic phase and predict their structural and magnetic properties. For all cases, the bulk moduli and spin susceptibilities are calculated and reported.

The paper is organized as follows. In Sec. II we outline the method and details of calculations, in Sec. III we discuss the self-consistent nonmagnetic results, and in Sec. IV the FSM results. Section V contains a summary.

II. METHOD

The calculations have been carried out using the well-known semirelativistic LMTO[13,14] method. The correction terms[14] were included. The c/a ratio has been set to the experimental values for the existing phases (Sc: 1.594, Ti: 1.588, Co: 1.622, and Fe: 1.54[2]) and to the ideal hcp value of $(\frac{8}{3})^{1/2}$ for the remaining elements (only these elements are referred to in the following as the hcp phases). 468 **k** points in the irreducible wedge of the Brillouin Zone have been used. The results presented below have been obtained in three steps.

(i) The self-consistent LMTO calculations of the electronic structure have been carried out for the nonmagnetic phase of every element as a function of atomic volume (20 to 30 atomic volumes have been considered for every element). The exchange-correlation potential of Vosko, Wilk, and Nusair[15] has been used.

(ii) The canonical scaling principle in the form including hybridization[16] has been used in order to obtain for every volume the electronic structure[17] of ferromagnetic phases with magnetic moments $M \neq 0$. The calculations have been carried out in the FSM mode, i.e., in every calculation the magnetic moment has been constrained to a predefined value. Note that it is *not* a rigid band model or a Stoner-like analysis of a sort used, e.g., in Ref. 6. The magnetic moment is used in the FSM method[8] as an input parameter which, together with the number of valence electrons, defines the Fermi energies for majority and minority spins. One starts from the nonmagnetic spin and state densities; the introduction of a nonzero magnetic moment changes the Fermi energies for both spins and hence the DOS moments. These in turn[14] allow us to calculate modified spin densities within the LMTO-ASA and then a new potential and new potential functions. They are used to scale the DOS again in order to obtain new moments. The whole procedure can now be iterated until self-consistency without diagonalization of the Hamiltonian. The procedure neglects the so called "differential hybridization," i.e., a difference in the degree of hybridization of sp and d bands for various magnetic moments. Judging from the earlier results[17] it is an excellent approximation, at least for elemental solids. Moreover, the procedure is extremely fast and one can easily afford to calculate the electronic structure for more than a thousand points in the M-V plane.

(iii) The basic quantities calculated from the FSM procedure are magnetic and mechanical equations of state [$H(M,V)$ and $p(M,V)$, respectively] as functions of magnetic moment M and atomic volume V (in the figures the atomic volume V is often replaced by the average Wigner-Seitz radius S_{WS}):

$$H(M,V)=[E_F^{\downarrow}(M,V)-E_F^{\uparrow}(M,V)]/2\mu_B \tag{1}$$

and[18]

$$p(M,V)=-\frac{1}{3V}\left[\sum_l\sum_\sigma\int^{E_F^\sigma} g_{l\sigma}(E)S\Phi_{l\sigma}^2(E)[D_{l\sigma}(E)+l+1][D_{l\sigma}(E)-1]dE\right.$$
$$\left.+\sum_l\sum_\sigma\int^{E_F^\sigma} g_{l\sigma}(E)S\Phi_{l\sigma}^2(E)[E-v(S)-\varepsilon_\sigma^{\mathrm{xc}}+v_\sigma^{\mathrm{xc}}]S^2dE\right], \tag{2}$$

where $g_{l\sigma}$ is the DOS for angular momentum l and spin σ, S is the Wigner-Seitz radius, $\Phi_{l\sigma}(E)$ is the radial wave function at S, $D_{l\sigma}$ is the logarithm derivative of Φ, $v(S)$ is the Coulomb potential at S, v_σ^{xc}, $\varepsilon_\sigma^{\mathrm{xc}}$ is the exchange-correlation potential and energy density, respectively.

The knowledge of these functions suffices for the calculation of the total energy $E(M,V)$ in two alternative ways: first, one can write the total energy $E(M,V)-E_0$ in the form of a Landau expansion

$$E(M,V)-E_0=\sum_{k=0}^{N}\sum_{j=0}^{N}a_{kj}V^kM^{2j}, \tag{3}$$

and then, forming $\partial(E-E_0)/\partial M$ and $-\partial(E-E_0)/\partial V$, carry out a simultaneous least-square fit of H and p. This procedure gives all the coefficients a_{kj} and hence the $E(V,M)$. The other way is to integrate the H and p functions:

$$E(V,0)-E_0=-\int_{V_0}^{V}p(V',0)dV' , \quad (4)$$

$$E(V,M)=E(V,0)+\int_0^M H(M',V)dM' , \quad (5)$$

in the manner of Hellman-Feynman theorem.[19] The latter method gives the possibility of an internal check of the theory: since we do not invest the information on the $p(M,V)$ for $M\neq 0$ in the calculations it is not trivial to calculate $p'(M,V)=-\partial E(M,V)/\partial V$ and compare it with the original $p(M,V)$. Such a check has been carried out and brought an excellent agreement, as illustrated below for the hexagonal Fe.

In the following we discuss several quantities like equilibrium Wigner-Seitz radii, the DOS at Fermi level, the Stoner exchange integral I, the Stoner product $Ig(E_F)$, the bulk modulus B_M, the molar spin susceptibility χ, and the susceptibility enhancement factor χ/χ_0 (χ_0-Pauli paramagnetic spin susceptibility). Several remarks seem to be necessary concerning the way these quantities have been calculated. Since we use a different exchange-correlation potential, the values of the Stoner integrals I have not been taken from the paper of Janak[12] but calculated for the equilibrium lattice constants from the FSM procedure using the expression

$$I=(C_d^{\downarrow}-C_d^{\uparrow}-2\mu_B H)/M , \quad (6)$$

where $C_d^{\downarrow\uparrow}$ are the mass centers of the majority and minority d bands (in general, I calculated in this way almost does not depend on M and is close to the values reported by Janak[12]). The total DOS $g(E_F)$ is given in (Ry cell)$^{-1}$, but the one used in the calculation of Stoner product is in (Ry at. spin)$^{-1}$. The molar susceptibility $\chi=dM/dH$ has been calculated self-consistently from the FSM procedure uniformly for $M=0.1\ \mu_B$ per atom. The susceptibility enhancement factor has been calculated from $\chi/\chi_0=(dM/dH)/\mu_B^2 g(E_F)$, where $g(E_F)$ is DOS in (Ry at.)$^{-1}$ (Ref. 20). We used also the perturbative formula[12]

$$\chi/\chi_0=[1-Ig(E_F)]^{-1} \quad (7)$$

and compared the results. The bulk moduli and the equilibrium lattice constants have been obtained by fitting the mechanical equation of state $p(V;M)$ by the Murnaghan[21] expression:

$$p(V;M)=\frac{B_M}{b}\left[\left(\frac{V_0}{V}\right)^b-1\right] . \quad (8)$$

This appears to be a very stable procedure which gives the χ^2 per point smaller than 1 kbar. Usually we have used 12 points around S_{WS} to fit $p(V)$. As a result, one obtains the atomic volume V_0, the bulk modulus at constant moment B_M, and the b parameter which describes the linear dependence of the bulk modulus on pressure: $B_M(p)=B_M(p=0)+bp(V)$. For the nonmagnetic phases $B_M=B_0$ is a measurable quantity, for the ferromagnetic phases one should actually calculate the bulk modulus at constant field $B_H=B_M/\eta$, where η-magnetovolume enhancement factor[22] which is usually of the order of 1–1.1. We estimate that the numerical error in finding the bulk modulus is not larger than 2–3 %.

III. SELF-CONSISTENT RESULTS FOR NONMAGNETIC PHASES

First, we wish to discuss the results of the self-consistent nonspin-polarized calculations. They are summarized in Table I and in Figs. 1 and 2. In Table I the equilibrium Wigner-Seitz radii, DOS at Fermi level, and the Stoner product are listed. In Figs. 1 and 2 the nonmagnetic state densities at equilibrium lattice constants are displayed. The energy scales have been shifted so that the Fermi energy falls at zero. A migration of the Fermi level through the multipeaked second maximum, the structureless valley above it and into the high and steep leading peak may be clearly observed. We note the following: the light transition metals Sc, Ti, and V fail the Stoner test and are nonmagnetic in the ground state. Nevertheless, Sc and V can be viewed as enhanced paramagnets, as opposed to Ti. Cr meets the Stoner criterion due to the fact that its Fermi energy falls exactly at the maximum of the central peak. Mn and Fe fail the Stoner test and are predicted to be nonmagnetic. Co and Ni fulfill the Stoner test and one expects a ferromagnetic instability to occur. Up to this point, our conclusions agree with those of Papaconstantopoulos, Fry, and Brener[11] and confirm their observation of the unusually high DOS at the Fermi level for the hcp Ni. Knowing the position of the Fermi energy with respect to the main features of the DOS curves we can, following the rules

TABLE I. Self-consistently calculated equilibrium Wigner-Seitz radii S_{WS} (a.u.), density of states at Fermi level $g(E_F)$ [(Ry cell)$^{-1}$], Stoner exchange integrals I (mRy), Stoner product $Ig(E_F)$ ($g(E_F)$-DOS in [(Ry atom spin)$^{-1}$], spin susceptibility χ (emu/mole), and susceptibility enhancement χ/χ_0. χ/χ_0 has been calculated from the FSM procedure as $(\partial M/\partial H)\mu_B^2 g(E_F)$ for $M=0.1\ \mu_B$.

Element	S_{WS}	$g(E_F)$	I	$Ig(E_F)$	χ	χ/χ_0
Sc	3.393	54.9	50	0.69	1.8×10^{-4}	2.75
Ti	3.042	24.4	47	0.30	5.5×10^{-5}	1.9
V	2.827	51.7	53	0.68	2.3×10^{-4}	3.75
Cr	2.670	74.1	60	1.11	<0	−4.5
Mn	2.588	31.8	60	0.48	1.1×10^{-4}	2.9
Fe	2.540	34.5	64	0.55	1.6×10^{-4}	3.95
Co	2.538	63.4	72	1.14	<0	−7.6
Ni	2.565	147.8	79	2.92	<0	−0.8

drawn by Moruzzi and Marcus[5] from the Stoner-like analysis of their self-consistent results for the bcc metals, explicate some predictions concerning the behavior of the 3*d* hexagonal phases upon the lattice expansion/compression. For Ti, with its Fermi level positioned left to the major peak of the DOS, a first-order transition of the type *II* is predicted. For Sc and V the Fermi levels fall within the third and second peaks, respectively. For these we expect second-order transitions of a type rather difficult to foresee, especially for V. Cr with its Fermi level at a local DOS maximum is a clear candidate for a second-order type-*I* transition. Since the Fermi levels for Mn and Fe are pinned in a deep DOS valley, first-order type-*II* transitions are expected. Finally, for Co and Ni one would expect second-order transitions probably of the type *I*. It should be noted the predictions for the hexagonal phases are in variance with those for the bcc ones[5] for Cr, Mn, and Fe: the bcc phases are expected to be nonmagnetic, low-spin, and ferromagnetic, respectively, whereas the predictions for the hexagonal phase are ferromagnetic (presumably with a low moment) for Cr and nonmagnetic for both Mn and Fe.

We have found that the number of *sp* electrons per atom for all elements amounts to 1.5 ∓ 0.1, in agreement with the general trends observed earlier.[23] This implies that the extra electrons added with growing atomic number are mainly of *d* character throughout the series. However, they do not screen completely the increasing nuclear charge. The mass center of the *d* bands is continuously lowering with increasing Z and the *d*-band width is decreasing dramatically at the end of the series. This effect leads to a very large DOS for hcp Ni, as reported by Papaconstantopoulos, Fry, and Brener.[11] The very same trend transforms the free-electron-like *d* bands of the early 4*d* transition metals into the semicore states at the end of the series.[24]

As we have mentioned, the calculated spin susceptibilities reported in Table I are based not on the perturbative formula (7) but on the self-consistent calculation of dM/dH. Moruzzi and Marcus[7] used the same procedure in order to calculate the susceptibilities for Rh and Pd. They found quite a good agreement with the data calculated according to Eq. (7). In some cases we also find such an agreement, in other cases however our self-consistent values differ by as much as 80%. We were not able to find any distinct pattern here. Our general experience with using Eq. (7) to find the critical S_{WS} values (the values at which the different magnetic phases show up or terminate) is that they are usually somewhat smaller than the values calculated self-consistently from the FSM method.

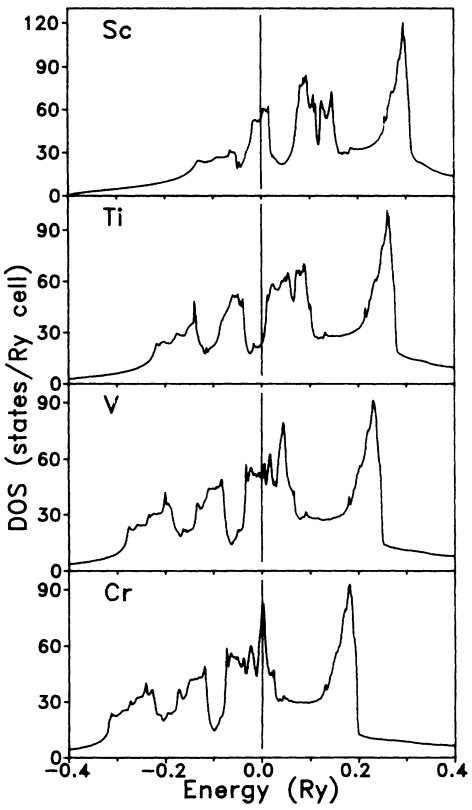

FIG. 1. DOS curves for nonmagnetic hexagonal phases of Sc, Ti, V, and Cr calculated at the equilibrium lattice constants (see Table I). Fermi level is placed at zero of the energy scale.

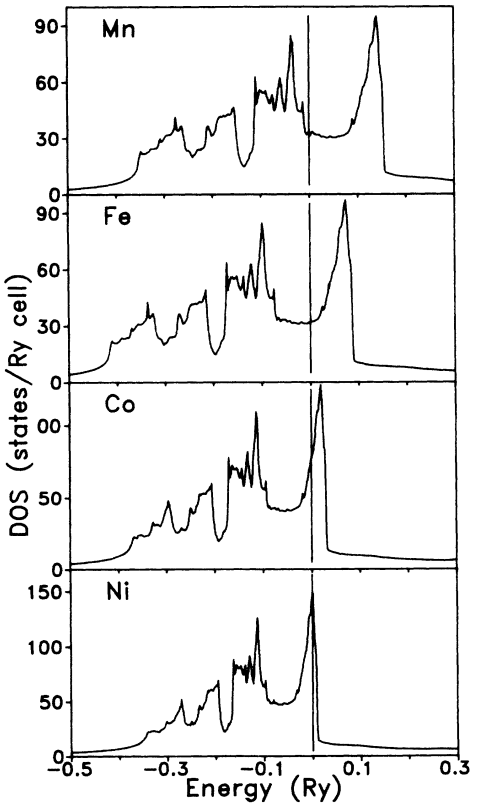

FIG. 2. DOS curves for nonmagnetic hexagonal phases of Mn, Fe, Co, and Ni calculated at the equilibrium lattice constants (see Table I). Fermi level is placed at zero of the energy scale.

TABLE II. Ground states, bulk moduli at constant magnetic moment B_M (Mbar), equilibrium (col. 2), and critical (col. 5) S_{WS} values (a.u.), and transition type according to classification of Moruzzi, Marcus, and Pattnaik (Ref. 4) for hexagonal 3d transition metals.

Element	S_{WS}	Ground state	B_M	Critical S_{WS}	Transition type
Sc	3.39	NM	0.67	4.15	*I*
Ti	3.04	NM	1.37	3.78, 4.03	*II*
V	2.83	NM	2.06	3.08	*I*
Cr	2.67	FM	2.77	2.67	*I*
Mn	2.59	NM	3.27	2.84, 3.04	*II*
Fe	2.54	NM	3.43	2.66, 2.85	*II*
Co	2.57	FM	2.80	2.33	*I*
Ni	2.57	FM	2.46	2.05	*I*

IV. SPIN-POLARIZED CALCULATIONS

The spin-polarized calculations have been carried out using both the FSM scheme and canonical scaling principle, as described in Sec. II. Following our computational strategy and keeping in mind the main goal of this study we illustrate our results mainly with the plots of the magnetic field $H(M;V)$ and electronic pressure $p(M;V)$. The $H(M;V)$ plots show the variation of the magnetic field $H(M)$ calculated from Eq. (1) for different lattice spacings. Such plots have been used by Shimizu[25] in his discussion of the metamagnetic behavior. The stable solutions are represented by $H=0$ points with $\partial H/\partial M>0$. For $M=0$ a negative slope of the $H(M)$ implies a ferromagnetic instability. We use in our discussion the $H(M)$ curves in place of frequently used $\bar{N}(M)$ curves.[26,5-7] The $p(M;V)$ curves are less interesting, following to the first order the quadratic dependence on the magnetic moment,[24] and will not be explicitly shown. Instead we chose an alternative way of displaying the crucial information using the combined $p(M,V)$ and $H(M,V)$ contour plots. The $H=0$ and $p=0$ contours have a special significance, the former being equivalent to the $M(V)$ curve. An intersection of the zero-pressure and zero-field contours gives the ground state of the system. For the cases of special interest the total energy will be discussed. All important numerical data are collected in Table II.

A. Hexagonal Sc, Ti, and hcp V

Of the light transition metals, Sc and Ti crystalize in a hexagonal structure. Their electronic structure has been recently studied by Blaha, Schwarz, and Dederichs.[10] Our results for the equilibrium lattice constant agree very well (Fig. 1). We extend the study of the electronic structure of Sc and Ti to the investigation of the onset of magnetism. The case of Sc is least interesting in this context and we refer to it here only for the sake of completeness. Sc shows the second-order type *I* onset of magnetism at $S_{WS}\cong 4.15$ a.u., as compared to the calculated and experimental[20] equilibrium S_{WS} values of 3.39 and 3.43 a.u., respectively. The bulk modulus of the hexagonal phase is very small, similarly as for the case of bcc Sc.[5] While the transition types are the same for hexagonal and bcc Sc,[5] the critical S_{WS} value for the hexagonal phase is much higher (4.15 a.u. as compared to 3.65 a.u. for the bcc phase).

The results for Ti are shown in Figs. 3 and 4. Figure 3 shows the $H(M)$ curves for different atomic volumes. Their shape indicates a metamagnetic behavior: with a growing atomic volume, the $H=0$ solution for a finite M shows up before a positive slope at $M=0$ disappears. The onset of magnetism is therefore of the first order and type *II*. This is better illustrated by the contour plot of $p(M,V)$ and $H(M,V)$ (Fig. 4). The ground state of hexagonal Ti is nonmagnetic with $S_{WS}=3.04$ a.u. in surprisingly good agreement with the experimental value of 3.05 a.u. The nonmagnetic phase is stable up to $S_{WS}=4.03$ a.u. and the ferromagnetic phase from $S_{WS}=3.78$ a.u. upward. This is of course of rather academic interest. The expansion of atomic volume requested for stabilization of the ferromagnetic phase is so large that the system would start to lose its cohesion first. As illustrated in Fig. 4 this might lead to a rather peculiar situation: the system would require a larger negative internal pressure for the state with a smaller volume and lower magnetic moment than for the one with a larger volume and larger moment. Comparing the hexagonal and bcc phases we note as for Sc an extended range of the nonmagnetic phase stability and transition of the type *II* rather than of the type *I*.[5]

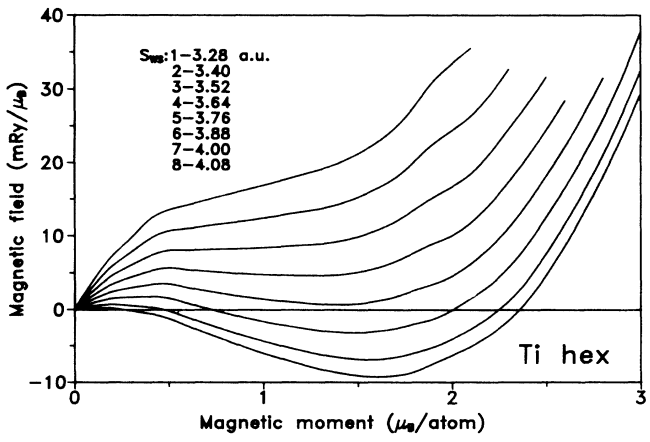

FIG. 3. Magnetic equations of state $H(M)$ of hexagonal Ti for several atomic volumes. The curves on this and all subsequent figures of this kind are numbered starting from the upper one.

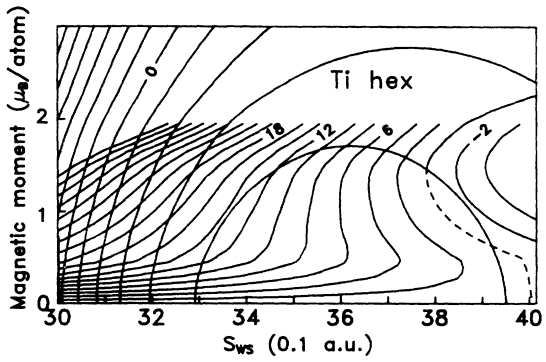

FIG. 4. The contour plot of magnetic and mechanical equations of state for hexagonal Ti. The field contours are plotted every 2 mRy/μ_B and the pressure contours every 50 kbar. The $H=0$ [$M(V)$] contour is plotted as a solid line in the accessible range and as a dashed line in the inaccessible range. The ground state is nonmagnetic with $S_{WS}=3.04$ a.u.

For hcp V we show only the contour plot of p and H. The ground state of this element is nonmagnetic with $S_{WS}=2.827$ a.u. The onset of magnetism seems to be of the second order and type I and the critical S_{WS} value is 3.08 a.u. The initial increase of the magnetic moment is so steep that we cannot definitely exclude a very narrow range of the coexistence of nonmagnetic and ferromagnetic phases. This is however of no practical importance. The $H=0$ contour (Fig. 5) shows a rather complicated $M(V)$ dependence without a sign of saturation for the considered volumes. The negative internal pressure required to stabilize a magnetic solution is approximately -300 kbar. We note again the important differences between hexagonal and bcc phases. The complicated type-*III* transition[5] for bcc V is replaced by a simple type-*I* transition. In general, as will be seen below, all the hexagonal elements except Co and Ni show qualitatively different magnetic behavior in hexagonal and bcc structures.

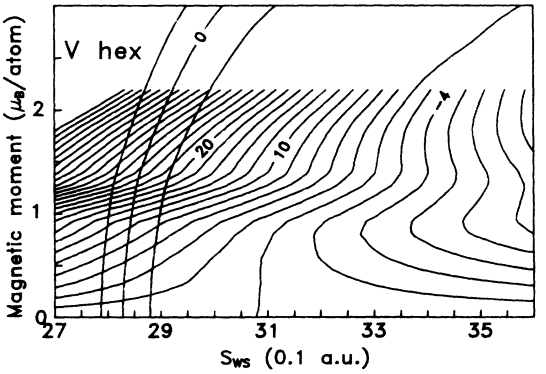

FIG. 5. The contour plot of magnetic and mechanical equations of state for hcp V. Field contours are plotted every 2 mRy/μ_B. For pressure, only -100, 0, and 100 kbar contours are shown. The ground state is nonmagnetic with $S_{WS}=2.83$ a.u.

B. hcp Cr

The hcp phase of chromium appears to be a special case. One can see from the data in Table I that the Stoner criterion is fulfilled. The Fermi level for the nonmagnetic phase is positioned just at the central peak. The $H(M)$ curves (Fig. 6) show a smooth onset of magnetism with the moment slowly increasing with atomic volume. From the contour plot of $H(M,V)$ and $p(M,V)$ (Fig. 7) one notices that the ground state of hcp Cr is ferromagnetic with the moment of ~ 0.12 μ_B per atom and $S_{WS}=2.67$ a.u. It appears therefore possible to produce a ferromagnetic hcp Cr at zero internal pressure. It should be noted that the equilibrium and the critical S_{WS} values for Cr almost coincide. Hence, the substrates forcing a smaller lattice spacing would quench the moment almost immediately, but these with a larger lattice spacing would increase it only marginally. In any case, an eventual successful epitaxial growth of hcp Cr might produce a weak itinerant ferromagnetism of the sort encountered hitherto only for compounds like $ZrZn_2$, Sc_3In, or $TcBe_{2-x}Cu_x$ containing the elements never known to exhibit a local-moment paramagnetism—a conclusion quite surprising for an element with the half-filled shell. It remains however a question whether an antiferromagnetic spin arrangement would not possess a lower total energy.

C. hcp Mn and hexagonal Fe

These two elements have both their Fermi levels positioned in the valley between the leading and the second peak of DOS and they both fail the Stoner test. Nevertheless, whereas the magnetic hcp Mn phase is not likely to be grown, the hexgaonal Fe constitutes a very interesting case. Beginning with Mn, the $p(M,V)$ and $H(M,V)$ contour plots are shown on Fig. 8. The ground state is nonmagnetic with $S_{WS}=2.59$ a.u. The $H=0$ contour shows the metamagnetic behavior at rather large lattice expansions. The range of the nonmagnetic and the ferromagnetic phase coexistence is quite large (2.85–3.01 a.u.) but the pressure required to reach the magnetic solu-

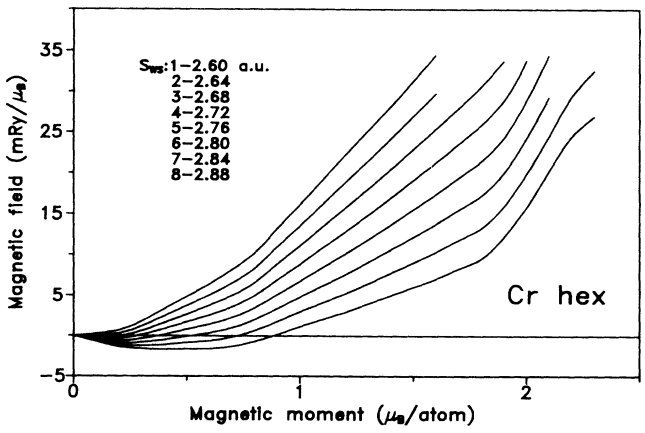

FIG. 6. Magnetic equations of state $H(M)$ of hcp Cr for several atomic volumes.

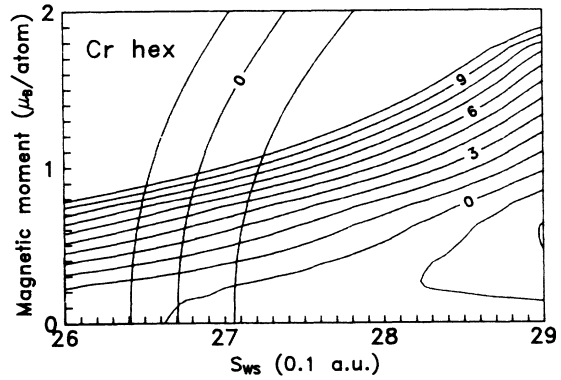

FIG. 7. The contour plot of magnetic and mechanical equations of state for hcp Cr. Field contours are plotted every 1 mRy/μ_B. For pressure, only -100, 0, and 100 kbar contours are shown. The ground state is ferromagnetic with $S_{WS}=2.67$ a.u. and $M=0.12\ \mu_B$. Note a small and slowly increasing magnetic moment.

tion is rather high and amounts to -150 kbar. The energy difference between the nonmagnetic and ferromagnetic phases is ~ 61 mRy. This is somewhat more than the 50 mRy reported by Moruzzi, Marcus, and Kübler[27] for fcc Mn. In this paper the authors also discuss the antiferromagnetic (AF) solutions for Fe and Mn. They have shown that for fcc Fe and Mn the onset of the AF phase coincides with the zero-pressure S_{WS}. The total energy $E(M)$ for the AF order may possess minima for $M\neq 0$ but $E(V)$ calculated along the stable AF branch is a monotonic function of atomic volume. This implies that although for both fcc Mn and Fe the AF solution has total energy lower than for the nonmagnetic case, there is no equilibrium solution ($p=0$) except for $M=0$. The pressure need not be zero for systems epitaxially clamped at volumes larger than equilibrium but it is obvious that clamping can be successful only for a moderate pressure and hence for small magnetic moments. We suppose that the essential features of the AF phases as calculated by Moruzzi, Marcus, and Kübler[27] for fcc Fe and Mn remain unchanged also for hexagonal phases. In such a case one might hope to obtain an AF phase of hcp Mn for the atomic volumes slightly larger than nonmagnetic equilibrium. For Cr the situation seems to be much more complicated due to the presence of ferromagnetic minimum at the onset and no trustworthy prediction concerning the AF phase can be made without explicit calculations.

As mentioned in the Introduction, the ferromagnetic hexagonal phase of Fe has recently been manufactured by Maurer *et al.*[2] Using classical technologies, the hexagonal Fe can only be obtained under a high pressure. The epitaxial growth, however, produces the ϵ-Fe with a rather large atomic volume which corresponds to the Wigner-Seitz radius of approximately 2.696 a.u. when extrapolated to a substrate-free ϵ phase. Maurer *et al.*[2] found that for more than four monolayers of the ϵ phase grown on the Ru substrate the material is ferromagnetically ordered with Fe atoms carrying a moment of approximately 2 μ_B. Such a moment compares surprisingly well with the equilibrium bcc Fe moment rather than with the fcc one at such a large atomic volume, despite the fact that the *NN* environment is the same in the fcc and hcp phases. This might suggest that the well-studied[3–6,28] fcc phase of Fe should not be used as a reference point when considering properties of the hexagonal phase.

We start the presentation of results for hexagonal Fe from the binding surface $E(M,V)$ (Fig. 9). It is topologically very similar to the binding surface of the fcc Fe calculated by Moruzzi, Marcus, and Kübler.[3] The minimum of $E(M,V)$ at $M=0$ and $S_{WS}=2.54$ a.u. clearly indicates a nonmagnetic ground state at nearly the same volume as for the fcc phase.[3] A characteristic "trough" at $S_{WS}\cong 2.65$ a.u. and $M\cong 2\ \mu_B$ is also there but, surprisingly, at the energy per atom almost twice as large as for the fcc phase.[3] This energy difference appears to be quite sensitive to the c/a ratio, growing when the c/a ratio decreases. The magnetic equation of state is shown in Fig. 10 for several atomic volumes varying by almost 20%. The curves are quite unusual: a positive slope at $M=0$

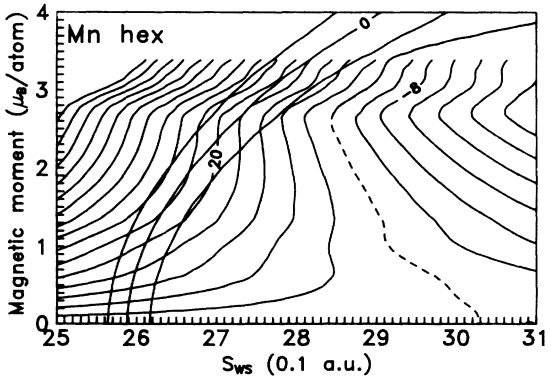

FIG. 8. The contour plot of magnetic and mechanical equations of state for hcp Mn. Field contours are plotted every 4 mRy/μ_B. For pressure, only -100, 0, and 100 kbar contours are shown. The ground state is nonmagnetic with $S_{WS}=2.59$ a.u.

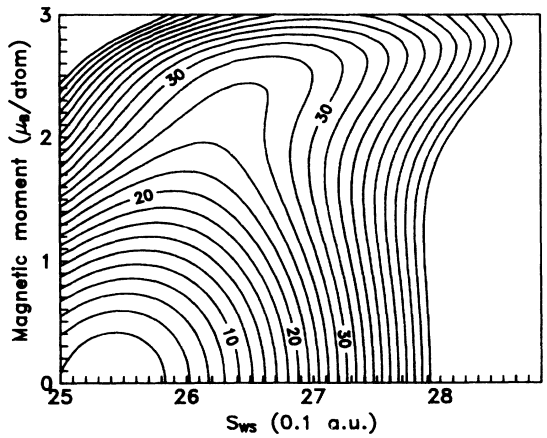

FIG. 9. Binding surface $E(M,S_{WS})$ (in mRy) for the hexagonal Fe with $c/a=1.54$.

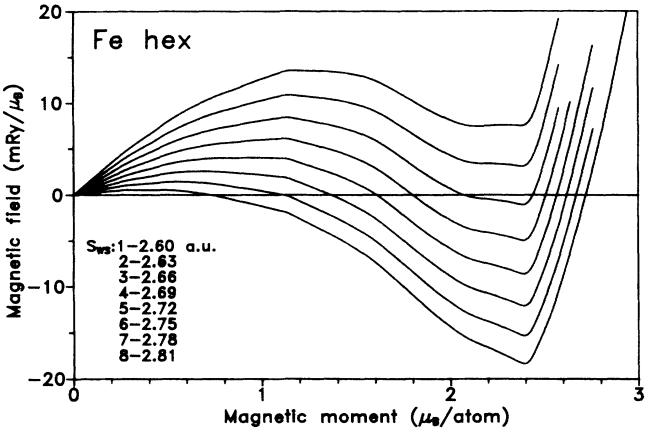

FIG. 10. Magnetic equation of state $H(M)$ of hexagonal Fe calculated for several lattice constants.

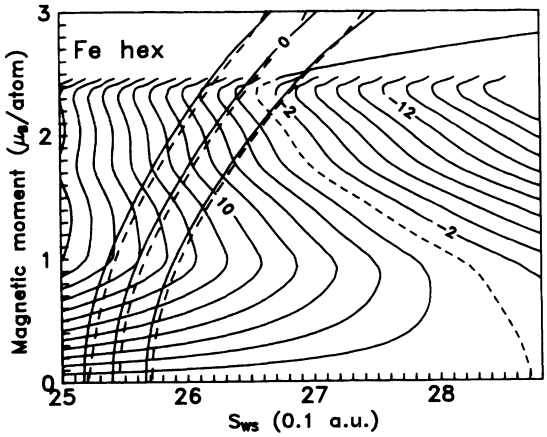

FIG. 11. Contours of the magnetic field $H(M,V)$ in mRy/μ_B for hexagonal Fe. Superimposed are contour lines of the $p(M,V)$ function, separated by 100 kbars. The proximity of the $p=0$ and $H=0$ lines at $S_{WS}\cong 2.66$ a.u. should be noted. The $p(M,V)$ contours are given here by solid and dashed lines. The solid lines represent the original $p(M,V)$ function, the dashed ones the $p'(M,V)$ function calculated by differentiation of the total energy surface calculated from Eqs. (4) and (5). The deviations at the upper edge are mainly due to the errors in numerical differentiation procedure.

extends up to $S_{WS}=2.85$ a.u. implying a film stability of the nonmagnetic phase at volume expansions as large as 20% of the equilibrium value. At the same time, however, already the $H(M)$ curve for $S_{WS}=2.66$ a.u. exhibits a metastable ferromagnetic phase with a moment of 2.42 μ_B per atom. Figure 11 shows the contour plot of the magnetic and mechanical equations of state. The nonmagnetic-ferromagnetic transition is similar to that found by Moruzzi, Marcus, and Kübler[3] for fcc Co but the range of a simultaneous stability of nonmagnetic and ferromagnetic phases is extremely large for hexagonal Fe and extends from $S_{WS}\cong 2.65$ a.u. to $S_{WS}\cong 2.85$ a.u. The behavior of the fcc and hexgonal phases of iron is quite different—the low-spin of the fcc Fe phase is absent for the ϵ phase and the metastability range is very large in the later case (in the fcc case it covers a small range of 2.66–2.685 a.u.). Figure 11 indicates also that the metamagnetic extension of the *HS* phase is possible down to and even below 2.5 a.u. The extremely large range of stability of the nonmagnetic phase of the hexagonal Fe is probably a reason why the solid solution Ru_xFe_{1-x} remains nonmagnetic in the whole range of stable concentrations.[2]

An origin of such a behavior of the hexagonal Fe can be easily traced back to the DOS shape. As seen in Fig. 2 for the hexagonal phase the Fermi level is positioned well within a broad, almost structureless plateau between two large maxima, whereas in the fcc case[28] it is placed at a slope of a smaller maximum. For the fcc phase this maximum in the *minority* spins DOS is placed above the Fermi energy for the high-spin and below it for the low-spin phase [see Fig. 2(a) in Ref. 28]. For the hexagonal phase, a lack of any additional structure in DOS between first two main peaks makes an appearance of a low-spin phase impossible.

The high-moment part of the $M(V)$ curve begins at $S_{WS}\cong 2.65$ a.u. with the moment of $\sim 2.4\ \mu_B$. The $M(V)$ curve is almost linear in this range with $d(\ln M)/dp$ equal to -4.7×10^{-4} kbar^{-1}. The calculated magnetic moment at the onset of the high-spin phase is already larger than the reported one.[2] The value at $S_{WS}=2.72$ a.u., corresponding to the atomic volume 12.5 Å^3, is even larger and equals 2.56 μ_B. Therefore, the observation of a relatively small moment in the hexagonal Fe cannot be explained. The calculated moment of the hexagonal phase is even larger then that expected for the fcc one at a comparable atomic volume. Figure 12 shows the ferromagnetic DOS at the experimentally observed volume. It is a DOS of a typical strong ferromagnet, with no holes in the majority spin band and also the calculated value of $\partial(\ln M)/\partial p$ is typical for strong ferromagnets. It seems that in order to explain the observed value of the magnetic moment the electronic structure calculations for thin film geometry might be necessary.

Failing, as they do, to explain the value of the magnetic moment of the hexgaonal Fe films, our calculations are more successful in the explanation of the very existence of the ferromagnetic state. The total energy curve (Fig. 13) plotted as a function of magnetic moment for $S_{WS}=2.72$ a.u. has a local minimum for a high moment. The energy at the local minimum is only marginally higher than at the minimum for $M=0$ and an increase of S_{WS} by a fraction of percent reverses the situation. Figure 13 shows also the total energy calculated along the $M(V)$ curves (i.e., for zero magnetic field) for nonmagnetic and ferromagnetic phases. The calculated total energy of the ferromagnetic phase becomes lower than that of the nonmagnetic one at $S_{WS}\cong 2.72$ a.u. Moreover, the slope of the $E(S_{WS})$ curve for the ferromagnetic phase is small at this point, implying a rather low negative internal pressure. This aspect is also illustrated in Fig. 11 where the $H=0$ and $p=0$ contours almost touch. The actual pressure calculated at $S_{WS}=2.72$ a.u. equals -140 kbar; taking however into account the usual $\sim 1.5\%$ overbinding, typical for all LSDA calculations, we estimate the strain of the ϵ-Fe layers epitaxially grown

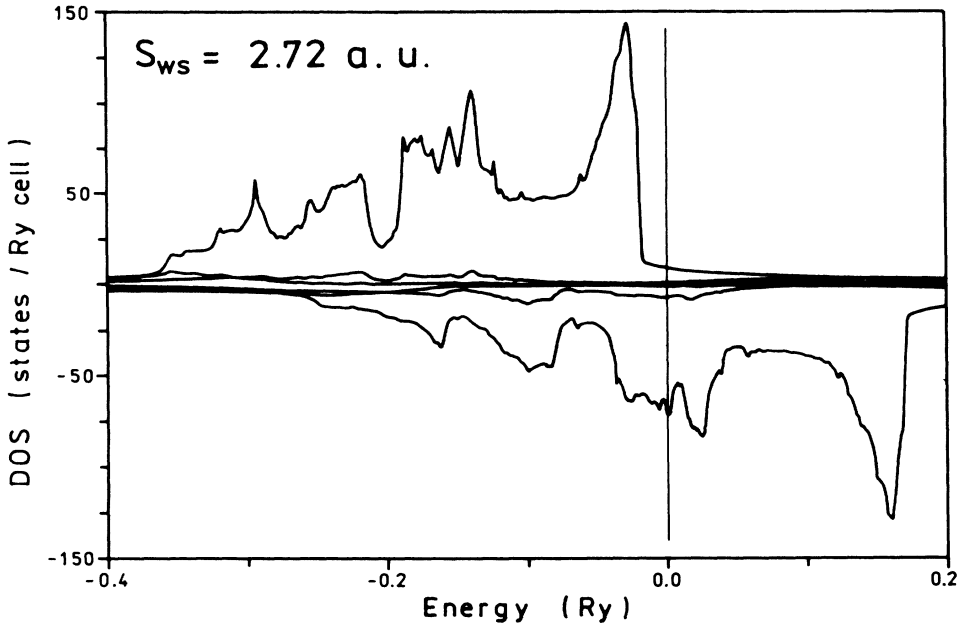

FIG. 12. Ferromagnetic DOS curves for the hexagonal Fe for $S_{WS}=2.72$ a.u. s, p, and d contributions are indicated.

on Ru substrate for approximately -70 kbar.

For Fe one should in principle also consider the AF phase. Under the assumptions discussed for Mn, a F-AF transition for Fe at $S_{WS}=2.72$ a.u. would end up in a destabilizing high-pressure situation. We believe, however, that also for hexagonal Fe one cannot exclude a small-moment AF phase at atomic volumes slightly larger than nonmagnetic equilibrium.

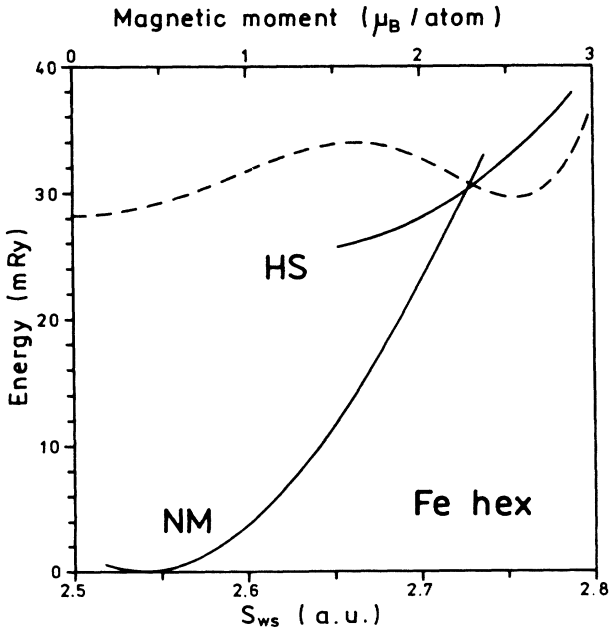

FIG. 13. Total energy for hexagonal Fe calculated along the $M(V)$ curve, i.e., at zero magnetic field (solid lines) and total energy as a function of magnetic moment for $S_{WS}=2.72$ a.u. (dashed curve).

D. Hexagonal Co and hcp Ni

The native form of Co is a hexagonal structure. The experimental values for the lattice constant a and for c/a ratio are[20] 2.51 Å and 1.622, respectively, and the magnetic moment equals to 1.6 μ_B.[29] These values of a and c/a correspond to $S_{WS}^{eq}=2.604$ a.u. In Fig. 2 one can see that the Fermi level falls left to the leading peak. The contour plot of H and p (Fig. 14) indicates the ferromagnetic ground state with $S_{WS}=2.568$ a.u. and $M=1.55$ μ_B. These values are in fair agreement with experiment. The calculated S_{WS}^{eq} is much closer to the experiment than the value reported by Jarlborg and Peter,[9] probably due to the different exchange-correlation potential used in this study. The $M(V)$ curve shows that the onset of magnetiza-

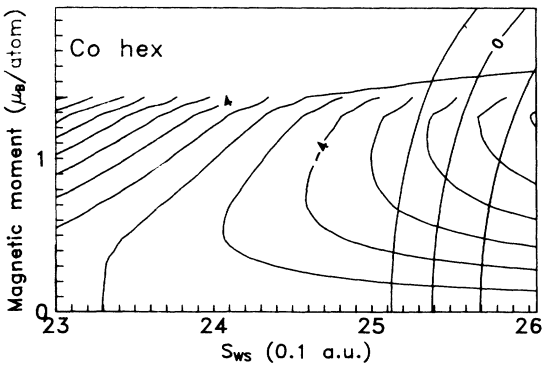

FIG. 14. The contour plot of magnetic and mechanical equations of state for hexagonal Co. Field contours are plotted every 2 mRy/μ_B. For pressure, only -100, 0, and 100 kbar contours are shown. The ground state is ferromagnetic with $S_{WS}=2.57$ a.u. and $M=1.55$ μ_B.

tion curve changes its slope at 1.4 μ_B, i.e., after the material undergoes the transition from a weak to strong ferromagnetism. In Fig. 15 we show the binding surface for the hexagonal Co. This result supplements the results of Moruzzi *et al.*[30] who calculated the binding surfaces for fcc and bcc phases of Co. The hexagonal surface has the saddle point approximately 9 mRy above the ferromagnetic minimum. This is less than one-half of the bcc value and 50% more as the fcc difference.[3] A trend in going from the fcc to the hexagonal phase is the same as for Fe and Mn.

The DOS for the ferromagnetic phase is very similar to the DOS calculated in Ref. 9 and will not be discussed here.

The last element considered in this paper is hcp Ni. As already noted by Papaconstantopoulos, Fry, and Brener,[11] it has an extremely large DOS at Fermi level (Fig. 2) and represents a case of strong ferromagnetism. This very large value is caused not only by the Fermi level falling exactly at the maximum of the leading peak but also by a relatively small band width, as discussed in Sec. III. The $H(M)$ curves (not shown) depend weekly on the atomic volume around the equilibrium value. The contour plot (Fig. 16) indicates the global equilibrium point at $S_{WS}=2.567$ a.u. and $M=0.59\ \mu_B$. The self-consistent calculations carried out by Papaconstantopoulos, Fry, and Brener[11] for $S_{WS}=2.59$ a.u. gave a huge moment of 0.76 μ_B. We cannot confirm this value. As for every strong ferromagnet the $M(V)$ curve has a rather small slope and according to our calculations an enormous lattice expansion would be needed to reach such a large moment. For Fe and Co we did not observe any substantial increase of the moment in going from the fcc to the hexagonal phase either. Since the different exchange-correlation potential can hardly account for the reported difference, we do not understand the value of the magnetic moment reported in Ref. 11. We suspect that it is an artifact caused by a small number of **k** points used in the self-consistent APW calculations and/or by the tight-binding interpolation scheme.

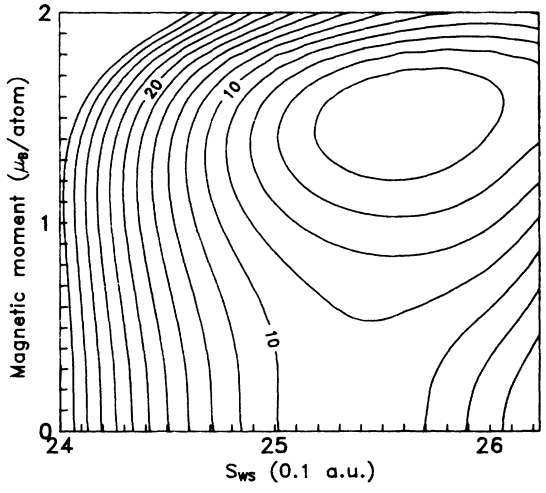

FIG. 15. Binding surface $E(M,S_{WS})$ (in mRy) for the hexagonal Co with $c/a=1.622$. Contours are plotted every 2 mRy.

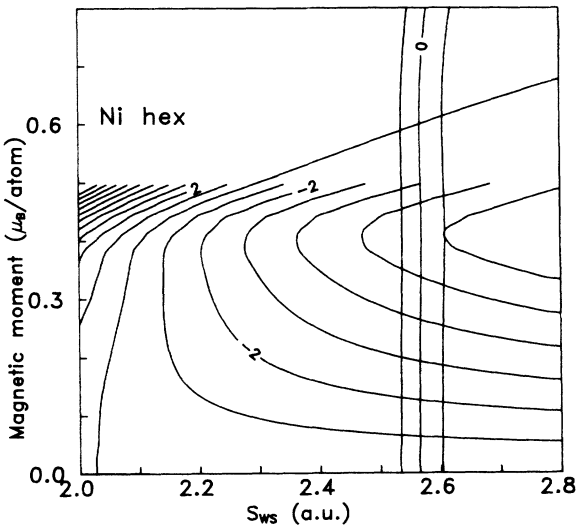

FIG. 16. The contour plot of magnetic and mechanical equations of state for hcp Ni. Field contours are plotted every 1 mRy/μ_B. For pressure, only −100, 0, and 100 kbar contours are shown. The ground state is ferromagnetic with $S_{WS}=2.57$ a.u. and $M=0.59\ \mu_B$.

A characteristic feature of the hcp Ni is a minimal spontaneous volume magnetostriction. This has been observed already for other phases of Ni.[3] The energy difference between the ferromagnetic minimum and the nonmagnetic saddle point is 2.2 mRy. The calculated equilibrium Wigner-Seitz radius is close to the fcc value and the range of stability of the ferromagnetic phase is very large. Hence, the hcp phase of Ni, if epitaxially grown, will surely be strongly ferromagnetic.

V. SUMMARY

We have calculated self-consistently the electronic structure and ground-state properties of all 3*d* metals in the hexagonal phase. The FSM method has been used in order to calculate the magnetic and mechanical equations of state and the total energy as a function of both magnetic moment and atomic volume. Although we do not consider any thin film geometry, we believe to have formulated the guidelines for MBE engineers. Accordingly, we suggest the following.

(i) The hexagonal phases of the light transition metals (Sc, Ti, V) and Mn are not likely to become ferromagnetic.

(ii) Cr is expected to be weekly ferromagnetic for any $S_{WS}>2.67$ a.u.

(iii) Fe is expected to be ferromagnetic at considerable lattice expansion but at low internal pressure. These findings have already been confirmed experimentally.[2] Hoever, the theory predicts a higher magnetic moment than that found experimentally.

(iv) For Co, the calculations gave ground-state properties in good agreement with experiment. The binding surface was calculated for the first time.

(v) hcp Ni is expected to be strongly ferromagnetic if grown on almost any substrate. We predict the magnetic moment comparable to the fcc moment.

(vi) For Mn, Fe, and Cr one cannot exclude a possibility of an AF spin ordering. For Cr we venture no prediction without explicit calculations. Taking into account the results of Ref. 27, we believe that for Mn and Fe only AF phases with small magnetic moments and a lattice spacing slightly larger than nonmagnetic equilibrium might be possible.

For all systems, the bulk moduli and the spin susceptibilities have been calculated as well as the art and conditions of the magnetic transitions discussed. A general behavior of the hexagonal phases seems to be simpler than that observed for the bcc or fcc phases. For hexagonal phases only *I* and *II* type transitions have been identified and no low-spin phases have been found.

ACKNOWLEDGMENTS

This work was partially supported by Deutsche Forschungsgemeinschaft under the project "Sonderforschungsbereich 166 Duisburg—Bochum" and by Polish Academy of Science Grant No. CPBP 01-12-4-14. We also acknowledge the financial support of the PAoS Grant No. CPBP 01-04-2-11, which enabled us to purchase a transputer system on which all the calculations were carried out. One of us (M.P.) thanks Professor W. Pepperhoff, whose continuous interest in the problem of electronic structure of the ϵ phases of 3*d* transition metals stimulated this study.

[1]G. A. Prinz, Phys. Rev. Lett. **54**, 1051 (1985).
[2]M. Maurer, J. C. Ousset, M. Piecuch, M. F. Ravet, and J. P. Sanchez, J. Mater. Res., in press; M. Maurer, J. C. Ousset, M. Piecuch, and M. F. Ravet, Europhys. Lett. **9**, 803 (1989).
[3]V. L. Moruzzi, P. M. Marcus, K. Schwarz, and P. Mohn, Phys. Rev. B **34**, 1784 (1986).
[4]V. L. Moruzzi, P. M. Marcus, and P. C. Pattnaik, Phys. Rev. B **37**, 8003 (1988).
[5]V. L. Moruzzi and P. M. Marcus, Phys. Rev. B **38**, 1613 (1988).
[6]G. L. Krasko, Phys. Rev. B **36**, 8565 (1987).
[7]V. L. Moruzzi and P. M. Marcus, Phys. Rev. B **39**, 471 (1989).
[8]A. R. Williams, V. L. Moruzzi, J. Kübler, and K. Schwarz, Bull. Am. Phys. Soc. **29**, 278 (1984); K. Schwarz and P. Mohn, J. Phys. F **14**, L129 (1984).
[9]T. Jarlborg and M. Peter, J. Magn. Magn. Mater. **42**, 89 (1984).
[10]P. Blaha, K. Schwarz, and P. H. Dederichs, Phys. Rev. B **38**, 9368 (1988).
[11]D. A. Papaconstantopoulos, J. L. Fry, and N. E. Brener, Phys. Rev. B **39**, 2526 (1989).
[12]J. F. Janak, Phys. Rev. B **16**, 255 (1977).
[13]O. K. Andersen, Phys. Rev. B **12**, 3060 (1975).
[14]H. L. Skriver, *Solid State Sciences* (Springer, Berlin, 1984), Vol. 41.
[15]S. H. Vosko, L. Wilk, and M. Nusair, Can. J. Phys. **52**, 1200 (1980).
[16]O. K. Andersen, W. Klose, and H. Nohl, Phys. Rev. B **17**, 1209 (1978).
[17]M. Podgorny, Physica **B161**, 105 (1989).
[18]N. E. Christensen and V. Heine, Phys. Rev. B **32**, 6145 (1985).
[19]P. H. Dederichs, S. Blügel, R. Zeller, and H. Akai, Phys. Rev. Lett. **53**, 2512 (1984).
[20]N. W. Ashcroft and N. D. Mermin, *Solid State Physics* (Holt, Rinehart and Winston, New York, 1976), p. 662.
[21]F. D. Murnaghan, Proc. Natl. Acad. Sci. U.S.A. **80**, 244 (1944).
[22]M. Shimizu, J. Phys. Soc. Jpn. **44**, 397 (1978).
[23]A. P. Malozemoff, A. R. Williams, and V. L. Moruzzi, Phys. Rev. B **29**, 1620 (1984).
[24]O. K. Andersen, O. Jepsen, and D. Glötzel, in *Highlights in Condensed Matter Theory,* edited by F. Bassani, F. Fumi, and M. Tosi (North-Holland, New York, 1985).
[25]M. Shimizu, J. Phys. (Paris) **43**, 155 (1982).
[26]O. K. Andersen, J. Madsen, U. K. Poulsen, O. Jepsen, and J. Kollar, Physica **86-88B**, 249 (1977).
[27]V. L. Moruzzi, P. M. Marcus, and J. Kübler, Phys. Rev. B **39**, 6957 (1989).
[28]M. Podgórny, J. Magn. Magn. Mater. **78**, 352 (1989).
[29]*AIP Handbook,* 2nd ed. (McGraw-Hill, New York, 1963).
[30]V. L. Moruzzi, P. M. Marcus, K. Schwarz, and P. Mohn, J. Magn. Magn. Mater. **54-57**, 955 (1986).